



OPEN Efficacy of antimicrobial photodynamic therapy with chitosan nanoparticles for decontamination of dental implants contaminated with *Aggregatibacter actinomycetemcomitans*

Ferena Sayar^{1✉}, Mohammad Reza Karimi^{1✉} & Sepehr Boroujerdi²

This study aimed to assess the efficacy of antimicrobial photodynamic therapy (aPDT) with chitosan nanoparticles (CNPs) for decontamination of dental implants inoculated with *Aggregatibacter actinomycetemcomitans* (*A. actinomycetemcomitans*). In this *in vitro* study, CNPs containing indocyanine green (ICG) were synthesized and characterized. Sandblasted large-grit acid-etched (SLA) titanium implants ($n=54$) were inoculated with *A. actinomycetemcomitans*, and randomly assigned to 6 groups ($n=9$) for decontamination: (I) negative control (PBS rinse for 60 s), (II) positive control [exposure to 0.2% chlorhexidine (CHX) for 5 min], (III) exposure to 0.25 mg/mL ICG at 37 °C for 5 min, (IV) exposure to 0.25 mg/mL ICG followed by 808 nm diode laser irradiation for 60 s, (V) exposure to 0.25 mg/mL ICG-loaded CNPs, (VI) exposure to 0.25 mg/mL ICG-loaded CNPs followed by 808 nm diode laser irradiation for 60 s. The *A. actinomycetemcomitans* colonies were counted, and data were analyzed by one-way ANOVA and Tamhane test ($\alpha=0.05$). The test groups showed a significant reduction in colony count compared to the negative control ($P<0.05$). Laser plus ICG-loaded CNPs and CHX had comparably the highest decontamination efficacy. This study demonstrated that aPDT with ICG-loaded CNPs significantly reduced the *A. actinomycetemcomitans* colony count on dental implants, showing comparable efficacy to CHX.

Keywords *Aggregatibacter actinomycetemcomitans*, Peri-implantitis, Photochemotherapy, Chitosan, Nanoparticles

Peri-implantitis is a common complication after implant treatment. It is an irreversible process characterized by bone loss ≥ 3 mm apical to the most¹ coronal portion of the intraosseous part of an implant, bleeding or pus discharge on probing, increased pocket depth (≥ 6 mm), pain and/or fistula^{1–6}. Microbial plaque accumulation around dental implants is the most important factor in pathogenesis of peri-implantitis⁷. In case of continuation and no treatment, peri-implantitis can lead to implant mobility and failure². The prevalence of peri-implantitis ranges from 13 to 26%⁸.

The most important steps in treatment of peri-implantitis include elimination of bacterial biofilm with minimal or no damage to the implant surface, detoxification of bacterial products, controlling the inflammatory reactions, and regaining osseointegration⁹. Although the clinical guidelines of the European Federation of Periodontology about the treatment of peri-implantitis mainly focus on non-surgical treatment, and suggest surgical approach as the next option, research is ongoing to find non-invasive modalities for this purpose, which are better accepted by both dental clinicians and patients¹⁰.

¹Department of Periodontics, Faculty of Dentistry, Tehran Medical Sciences, Islamic Azad University, Tehran, Iran.

²Tehran, Iran. ✉email: sayar_f@yahoo.com; mrkarimip@hotmail.com

Elimination of biofilm from the implant surface can be achieved by several chemomechanical methods (periodontal cures, ultrasonic instruments, air-powder abrasion, and citric acid) as well as systemic antibiotic therapy¹¹. The conventional techniques have shortcomings such as altering the implant surface, generation of bacterial resistance, and limitations in complete microbial plaque removal¹². Laser irradiation and antimicrobial photodynamic therapy (aPDT) were also recently suggested for treatment of peri-implantitis⁹.

Following its successful application for treatment of periodontitis, aPDT was suggested for elimination of bacteria in treatment of peri-implantitis¹³. Antimicrobial PDT is a photo-chemical decontamination technique operating based on activation of a photosensitizer with laser light and subsequent generation of cytotoxic reactive oxygen species, which are toxic for bacterial cells and can eliminate them. The light required for activation of photosensitizer should have a specific color and wavelength⁷. Previous studies reported different effects of aPDT as an adjunct for treatment of peri-implantitis^{7,14–16}. Also, aPDT is a safe and non-invasive method that does not damage the implant surface^{7,17,18}. Nonetheless, the conventional aPDT has limitations as well. For instance, its efficacy is limited to light-accessible areas, which are usually smaller than few tens of millimeters. Due to this limitation, aPDT can only be used for surface or subsurface lesions, as in skin cancers, and it is not favorably effective for deeper lesions. Also, photosensitizers may accumulate and cause tissue damage following light exposure. Furthermore, molecular oxygen should be necessarily present in order for the aPDT to exert its effect; while, some lesions are hypoxic and have low oxygen levels, which may lower the efficacy of aPDT. Furthermore, application of photosensitizers can make the skin and eyes super-sensitive to light for a relatively long period of time, which is another drawback of aPDT¹⁹.

A recent systematic review and meta-analysis showed that adjunctive aPDT had insignificant clinical efficacy compared with mechanical debridement alone for non-surgical treatment of peri-implantitis, and reported that complete resolution of peri-implantitis with non-surgical periodontal therapy was unpredictable²⁰. Also, the currently available photosensitizers are not ideal. They have inadequate therapeutic penetration depth and poor water insolubility²¹.

The aforementioned limitations in the efficacy of aPDT highlight the need for new photosensitizers with favorable antibacterial properties to improve the clinical outcomes of treatment of peri-implantitis with aPDT^{19,21}.

Application of nanoparticles (NPs) may be able to eliminate the current challenges of aPDT and improve its performance. Small size and large contact area increase the efficacy of NPs and prevent the accumulation of photosensitizer in areas far from the target site, and enhance the efficacy of free radicals as such. Also, NPs can accumulate closer to the target site due to their increased permeability while preserving their effect. NPs can also improve the water solubility of photosensitizers and enhance the delivery of the required dose of photosensitizer to the target site with minimal damage to the adjacent tissues²². Moreover, NPs can minimize the photodegradation of photosensitizer during delivery and fast dispersion at the target site²².

Considering the superior penetration depth of 808 nm diode laser in deep tissues and consequently superior regeneration and repair of injured host cells, indocyanine green (ICG) is an appropriate photosensitizer for aPDT. It is a non-toxic anionic cyanine-type photosensitizer. However, instability is its main drawback. It has high water solubility and highly absorbs 810 nm wavelength. The negative charge of the bacterial outer membrane affects the attachment of ICG and its efficacy as a photosensitizer in aPDT. Slight contraction of ICG due to this negative charge may reduce the binding to microorganisms and hinder its efficacy as a photosensitizer in aPDT²³.

Chitosan nanoparticles (CNPs) have several advantages such as biodegradability, no toxicity, and low immunogenicity. The positive charge of CNPs neutralizes the negative charge of ICG, causing better contraction of ICG²³. According to previous studies, CNPs, as a cationic amino-polysaccharide and a water-soluble polymer, have ideal properties for delivery of photosensitizers in aPDT^{24,25}. Although the benefits of aPDT in treatment of peri-implantitis have been well documented in the literature^{26,27}, the efficacy of application of CNPs as a carrier for ICG remains to be elucidated. Thus, this study aimed to assess the efficacy of aPDT with CNPs for decontamination of dental implants inoculated with *Aggregatibacter actinomycetemcomitans* (*A. actinomycetemcomitans*) as one of the microorganisms isolated from the peri-implantitis biofilm^{7,28}. We hypothesize that aPDT with ICG-loaded CNPs will result in a more significant reduction in *A. actinomycetemcomitans* colony count compared to conventional treatments, such as chlorhexidine (CHX).

Materials and methods

This in vitro experimental study was conducted on 54 sandblasted large-grit acid-etched (SLA) titanium implants purchased from ACH Medical Company (G. DIFF Implant; ACH Medical Co. Republic of Korea) with 4.5 mm diameter and 14 mm length contaminated with *A. actinomycetemcomitans*. Only one type of photosensitizer (ICG) and one single bacterial species (*A. actinomycetemcomitans*) were used in this study to focus specifically on photodynamic interaction under standardized conditions.

Sample size

The minimum sample size was calculated to be 9 in each group according to a previous study by Sayar et al.²⁹, and assuming $\alpha=0.05$, $\beta=0.2$, mean standard deviation of the percentage of reduction in colony count to be 11.26, and effect size of 0.61 using one-way ANOVA power analysis of PASS 11.

Synthesis of ICG-loaded CNPs

ICG-loaded CNPs were synthesized by the microfluidic method as thoroughly explained elsewhere³⁰. The drug loading efficiency was 3.51%.

Characterization of ICG-loaded CNPs

As explained elsewhere³⁰, the morphology and nanoscale size of CNPs were determined by scanning electron microscopy (Seron Technology, Korea) and dynamic light scattering (Zetasizer, Malvern, UK). Also, visible-ultraviolet spectrophotometry (Shimatzo, Japan) was performed to determine the loading of ICG onto CNPs³¹.

A. actinomycetemcomitans biofilm formation on titanium implants

SLA titanium implants with 4.5 mm diameter and 14 mm length were purchased from Biogenesis GDIFF ACH Medical Company (Biogenesis GDIFF ACH Medical Co., Republic of Korea). *A. actinomycetemcomitans* (ATCC33384) was obtained from the Microbiology School of Tehran University of Medical Sciences in lyophilized form, and cultured on tryptic soy agar containing 3% yeast extract. It was then incubated in an anaerobic jar (anaeroPack/CO₂) with 5% CO₂ at 37 °C for 48 h²⁸. The implants were inoculated with 1 mL of *A. actinomycetemcomitans* bacterial suspension with a final concentration of 10⁷ colony forming units (CFUs)/mL in tryptic soy broth and incubated in an anaerobic jar with 5% CO₂ at 37 °C²⁸. The implants were then rinsed with 5 mL of sterile phosphate buffered saline (PBS) to eliminate planktonic bacteria. The implants were then randomly assigned to 6 groups as follows (*n* = 9):

Group I: Inoculated implants did not undergo any intervention. They were only rinsed with sterile PBS for 60 s (negative control group).

Group II: Inoculated implants were rinsed with PBS for 60 s, and were then exposed to 0.2% chlorhexidine (Iran Najo, Tehran, Iran) for 5 min (positive control group).

Group III: Inoculated implants were rinsed with PBS for 60 s, and were then exposed to 0.25 mg/mL ICG³² for 5 min in the dark at 37 °C.

Group IV: Inoculated implants were rinsed with PBS for 60 s, and were then exposed to 0.25 mg/mL ICG for 5 min in the dark at 37 °C. Subsequently, they underwent diode laser irradiation (Konftec, New Taipei, Taiwan) with 808 nm wavelength, 250 mW power, and 29.85 J/cm² energy density with 8 mm tip at 1 mm distance from the implants for 60 s in a circular manner (the laser handpiece was held at 1 mm distance from the implant surface by using a base and a clamp. The implant was firmly held from the cover screw by a rotating rod connected to a small motor).

Group V: Inoculated implants were rinsed with PBS for 60 s, and were then exposed to 0.25 mg/mL ICG-loaded CNPs for 5 min in the dark at 37 °C.

Group VI: Inoculated implants were rinsed with PBS for 60 s, and were then exposed to 0.25 mg/mL ICG-loaded CNPs for 5 min in the dark at 37 °C. Subsequently, they underwent diode laser irradiation with 808 nm wavelength, 250 mW power, and 29.85 J/cm² energy density at 1 mm distance with 8 mm tip for 60 s in a circular manner.

Assessment of antibacterial activity

The implants were transferred into microtubes containing 1 mL of modified tryptic soy broth. To eliminate the biofilm from the implant surface, microtubes containing implants were sonicated (Sinaptec, Germany) with 50 Hz frequency and 150 W power for 30 s. Next, 10 µL of the suspension was transferred to a 96-well round-end micro-titer plate (TPP, Trasadingen, Switzerland) containing 90 µL of modified tryptic soy broth. After 10 times serial dilution, 100 µL of each concentration (dilution) was cultured on sheep blood agar plates, and the plates were incubated in an anaerobic jar at 37 °C and 5% CO₂ for 48 h.

The number of colonies in each group was then counted according to the method described by Miles et al.³³, and reported as CFUs/mL. The antimicrobial effect was determined by the percentage of reduction in colony count after culture. The microbiologist and the statistician were blinded to the treatments of the study groups.

Statistical analysis

Due to normal distribution of data as confirmed by the Shapiro-Wilk test ($P > 0.05$), the colony count among the groups was compared by one-way ANOVA followed by the Tamhane test for pairwise comparisons (due to non-homogeneity of the variances as shown by the Levene's test). $P < 0.05$ was considered statistically significant.

Results

Table 1; Fig. 1 present the measures of central dispersion for the colony count in the study groups. As shown, the highest colony count was noted in the negative control group followed by the ICG group, and the lowest colony count was found equally in aPDT with ICG-loaded CNPs and CHX groups. One-way ANOVA revealed a significant difference in colony count among the groups ($P = 0.000$). Pairwise comparisons by the Tamhane test (Table 2) showed that the colony count in the negative control group was significantly higher than that in all other groups ($P = 0.000$); it had the greatest difference with aPDT with CNPs, and the smallest difference with the ICG group. The colony count in the positive control group was significantly lower than that in the ICG group ($P = 0.011$). The colony count in the ICG group was significantly higher than that in aPDT with ICG-loaded-CNPs group ($P = 0.004$), and ICG-loaded CNPs ($P = 0.022$) groups. The colony count in the aPDT with ICG group was significantly higher than that in aPDT with ICG-loaded CNPs group ($P = 0.013$). The colony count in the ICG-loaded CNPs group was significantly lower than that in the ICG group ($P = 0.022$). Also, aPDT with ICG-loaded CNPs group showed significantly lower colony count than the ICG alone ($P = 0.004$). No other significant differences were found ($P > 0.05$).

The calculated logarithmic reduction values (relative to PBS) were as follows:

- CHX: $\log_{10}(66.78) - \log_{10}(1.47) = 1.824 - 0.168 = 1.656$ log reduction.
- ICG: $\log_{10}(66.78) - \log_{10}(5.18) = 1.824 - 0.714 = 1.110$ log reduction.
- PDT with ICG: $\log_{10}(66.78) - \log_{10}(2.80) = 1.824 - 0.447 = 1.377$ log reduction.

Group	Mean	Std. Deviation	Std. Error	95% Confidence Interval for Mean		Minimum	Maximum
				Lower Bound	Upper Bound		
PBS	66.7778	6.74125	2.24708	61.5960	71.9596	51.00	74.00
CHX	1.4667	0.46098	0.15366	1.1123	1.8210	0.80	2.10
ICG	5.1844	2.16071	0.72024	3.5236	6.8453	3.20	10.40
PDT with ICG	2.8000	1.10567	0.36856	1.9501	3.6499	1.60	5.00
ICG-loaded CNPs	1.8667	1.00499	0.33500	1.0942	2.6392	0.70	4.00
PDT with ICG-loaded CNPs	0.9667	0.62048	0.20683	0.4897	1.4436	0.30	2.30
Total	13.1770	24.39932	3.32033	6.5173	19.8368	0.30	74.00

Table 1. Measures of central dispersion for the colony count in the study groups ($n=9$). PDT: photodynamic therapy ICG: indocyanine green CNP: chitosan nanoparticles.

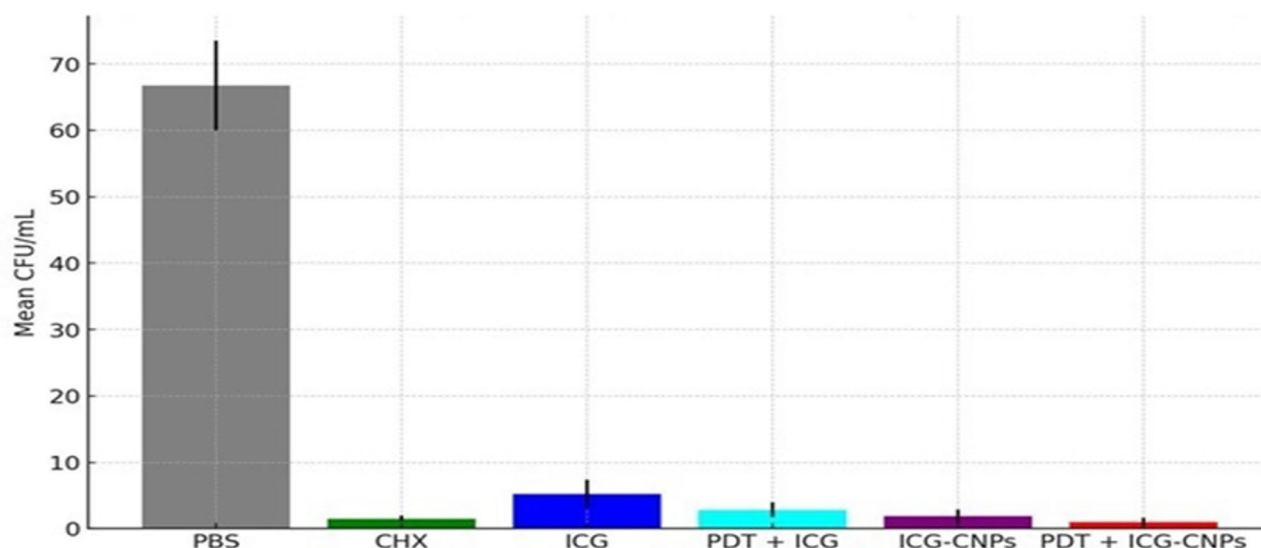


Fig. 1. Mean colony-forming Units (CFU/ml) PER treatment groups.

- ICG-loaded CNPs: $\log_{10}(66.78) - \log_{10}(1.87) = 1.824 - 0.272 = 1.552$ log reduction.
- PDT with ICG-loaded CNPs: $\log_{10}(66.78) - \log_{10}(0.97) = 1.824 - (-0.013) = 1.837$ log reduction.

The log reduction values demonstrated that PDT with ICG-loaded CNPs achieved the highest bacterial reduction (1.837 log), comparable to CHX (1.656 log reduction), and greater than ICG alone or PDT with ICG.

Figure 2 demonstrates the logarithmic reductions (\log_{10} CFU) in the experimental treatment groups.

Discussion

This study assessed the efficacy of aPDT with CNPs for decontamination of dental implants inoculated with *A. actinomycetemcomitans*.

Aside from the aforementioned limitations, conventional aPDT lacks bacteria-specific targets, which can result in off-target generation of heat and reactive oxygen species, damaging the healthy cells and compromising the efficacy of treatment. The efficacy of aPDT can be significantly enhanced by incorporating NPs as adjuvants. Targeted aPDT by using photosensitizers loaded with nanomaterials and modified with cationic groups or corresponding bacterial ligands may boost the efficacy of antibacterial therapy. NPs offer unique advantages due to their small size, large surface area, and their ability to be functionalized with various chemical groups^{19,21}.

The present results showed that aPDT with 808 nm diode laser and ICG-loaded CNPs significantly decreased the *A. actinomycetemcomitans* colony count compared to the negative control group. Also, the results indicated that use of aPDT and ICG photosensitizer also caused a significant reduction in colony count compared to the negative control group. Antimicrobial PDT with ICG-loaded CNPs showed the highest antimicrobial efficacy while ICG alone had the lowest antibacterial efficacy after the negative control group. This difference can be due to the antimicrobial activity of chitosan, increased contact surface area of photosensitizer when loaded onto

Group (I)	Group (J)	Mean Difference (I-J)	Std. Error	Sig.	95% Confidence Interval	
					Lower Bound	Upper Bound
PBS	CHX	65.31111 [*]	2.25233	0.000	56.0973	74.5249
	ICG	61.59333 [*]	2.35969	0.000	52.4945	70.6921
	PDT with ICG	63.97778 [*]	2.27711	0.000	54.8073	73.1483
	ICG-loaded CNPs	64.91111 [*]	2.27192	0.000	55.7325	74.0897
	PDT with ICG-loaded CNPs	65.81111 [*]	2.25658	0.000	56.6056	75.0166
CHX	ICG	-3.71778 [*]	0.73645	0.011	-6.6483	-0.7873
	PDT with ICG	-1.33333	0.39930	0.098	-2.8274	0.1608
	ICG-loaded CNPs	-0.40000	0.36856	0.995	-1.7620	0.9620
	PDT with ICG-loaded CNPs	0.50000	0.25766	0.672	-0.3972	1.3972
ICG	PDT with ICG	2.38444	0.80906	0.169	-0.5618	5.3307
	ICG-loaded CNPs	3.31778 [*]	0.79433	0.022	0.3877	6.2478
	PDT with ICG-loaded CNPs	4.21778 [*]	0.74935	0.004	1.2984	7.1371
PDT with ICG	ICG-loaded CNPs	0.93333	0.49805	0.711	-0.7791	2.6458
	PDT with ICG-loaded CNPs	1.83333 [*]	0.42262	0.013	0.3133	3.3534
ICG-loaded CNPs	PDT with ICG-loaded CNPs	0.90000	0.39370	0.451	-0.4988	2.2988

Table 2. Pairwise comparisons of the groups regarding colony count by the Tamhane test. *: significant at the 0.05 level.

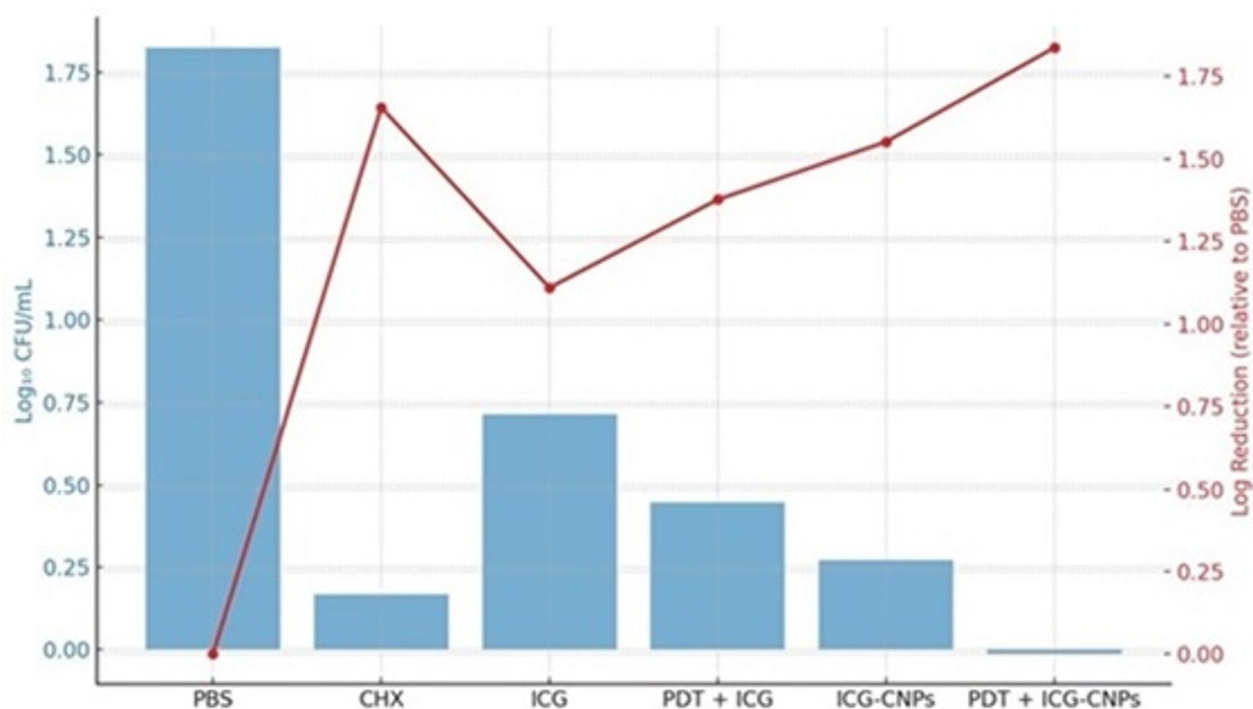


Fig. 2. Log₁₀ CFU and log reduction per treatment groups.

CNPs, and activation of photosensitizer with laser^{21,24}. Near infrared (NIR) light offers several advantages, such as improved biosafety and deeper tissue penetration. Resultantly, NIR-responsive photosensitizers have attracted considerable attention³⁴. ICG was used as the photosensitizer in the present study due to its optimal properties, acceptable light absorption in 700–800 nm wavelength (NIR spectrum), and maximum absorption at 800–810 nm wavelength²⁴. ICG offers considerable advantages with respect to biosafety and metabolic modalities. It has been clinically approved and is considered safe for use. ICG can generate abundant reactive oxygen species following

exposure to 808 nm NIR light, making it a promising candidate for NIR antimicrobial therapy³⁴. However, ICG has drawbacks such as very short circulatory lifetime, water instability, photodegradability, photobleaching properties, thermal degradation, and tendency to bind to lipoproteins, resulting in rapid clearance in vivo, limiting its clinical application^{23,34}. ICG photosensitizer has a negative charge. Thus, its encapsulation in CNPs, which are inexpensive, non-toxic, biodegradable, and a naturally occurring cationic polysaccharide, would enable ICG to easily bind to the bacterial cell membrane and increase its bactericidal effect^{23,29,35}.

Sayar et al.²⁹ assessed the effect of aPDT with toluidine blue and 635 nm diode laser, and ICG and 808 nm laser on *A. actinomycetemcomitans* biofilm formed on Laser-Lok titanium discs. They demonstrated that both protocols significantly decreased the bacterial biofilm compared to the control group. Their results were in line with the present findings; however, the present study was conducted on actual dental implants and CNPs were used as carriers for ICG, highlighting the optimal efficacy of aPDT with ICG for implant surface decontamination.

Rahman et al.¹⁸ demonstrated that application of aPDT did not alter the implant surface and effectively decreased the number of microorganisms involved in peri-implantitis, such as *A. actinomycetemcomitans*, *Porphyromonas gingivalis*, and *Prevotella intermedia*. Clinically, aPDT as an adjunct to mechanical debridement showed promising results in management of peri-implantitis at least in the short term¹⁸.

Shi et al.³⁵ evaluated the synergistic efficacy of aPDT and photothermal therapy with prefabricated NPs containing photosensitizer and a poly-cationic brush for treatment of periodontitis. They reported that NPs containing ICG and polycationic brush had excellent absorption in *Porphyromonas gingivalis* (involved in periodontitis), and was successful as a carrier for ICG. Moreover, the results showed that ICG-loaded polycationic brush + laser had the highest antibacterial efficacy while ICG and polycationic brush alone had the lowest antibacterial efficacy compared to the control group, which was in agreement with the present findings. It should be noted that NPs, particularly positively-charged NPs, play a role in increasing the efficacy of aPDT and reducing the adhesion of microorganisms, especially Gram-negative microorganisms, which are mainly responsible for periodontal disease. They paid special attention to the positive electric charge of NPs, which resulted in greater inhibition of Gram-negative microorganisms and synergistic effects with aPDT, which was similar to the effect of CNPs in the present study. Rad et al.²⁴ assessed the expression level of *rcpA* gene as a virulence factor involved in *A. actinomycetemcomitans* biofilm formation after aPDT using ICG-loaded CNPs. They showed that aPDT with ICG-loaded CNPs decreased the expression level of *rcpA* gene by 13.2 folds. Also, a significant difference existed in this respect between aPDT with ICG-loaded CNPs and ICG alone, which was similar to the present findings although they assessed gene expression while bacterial count was measured in the present study. Ghasemi et al.¹⁶ assessed the effects of aPDT with laser or light emitting diode (LED) compared with CHX on *A. actinomycetemcomitans* biofilm formed on titanium discs. They demonstrated that aPDT with LED and photosensitizer decreased the count of microorganisms on disc surfaces; nonetheless, colony count reduction was significantly greater in 0.2% CHX group. In the current study, aPDT with photosensitizer decreased the colony count. Also, aPDT with ICG-loaded CNPs caused a significantly greater reduction in colony count, comparable to the effect of CHX with no significant difference. Karimi et al.³⁶ assessed the effect of aPDT on SLA titanium discs inoculated with *Eikenella corrodens* and *A. actinomycetemcomitans*. The results revealed a significant reduction in colony count of both microorganisms following aPDT, compared with the negative control group; also, 0.2% CHX yielded a significantly lower colony count compared to aPDT. The present results indicated that application of positively charged CNPs along with aPDT and photosensitizer (ICG) was as effective as CHX (i.e., the gold standard) in reduction of *A. actinomycetemcomitans* count in vitro, which is a promising finding. Considering the cytotoxic effects of CHX on osteoblasts and host cells^{17,37,38}, it appears that using aPDT with ICG-loaded CNPs yields comparable, if not superior, antimicrobial results. This combination appears to be a better alternative to CHX, as it lacks the associated cytotoxicity. Therefore, it may serve as a safer option for clinical application in treatment of peri-implantitis.

It should be noted that Karimi et al.³⁶ used toluidine blue as the photosensitizer in their study and assessed titanium discs while ICG was used as the photosensitizer in the present study and dental implants were evaluated to better simulate the clinical setting. Nagahara et al.³⁹ evaluated the antibacterial activity of aPDT with ICG-loaded nanospheres as a new photosensitizer and 805 nm low-level diode laser against *Porphyromonas gingivalis*. They indicated that ICG-loaded nanospheres adhered to the surface of *Porphyromonas gingivalis*, and aPDT caused a significant reduction in *Porphyromonas gingivalis* count. Nonetheless, ICG + laser irradiation, laser irradiation alone, ICG alone, and ICG-loaded nanospheres alone had no significant effect on bacterial count. *Porphyromonas gingivalis* is a Gram-negative obligate anaerobe, and the electric charge of poly(lactic-co-glycolic) acid along with ICG was negative. Thus, the adopted aPDT protocol against *Porphyromonas gingivalis* was weaker compared to when CNPs are used. Addition of chitosan changes the electric charge to positive, resulting in greater antibacterial activity against Gram-negative microorganisms. The positive charge of ICG-loaded CNPs used in the present study and their different synthesis protocol may explain the difference between the present results and those of Nagahara et al.³⁹. Also, they used 0.05 mg/mL concentration of ICG while the ICG concentration was 0.25 mg/mL in the present study; this difference along with assessment of different microorganisms, and different time of colony counting (after 7 days in their study versus 48 h in the present study) may be other reasons for the variable results³¹. Divakar et al.⁴⁰ assessed the efficacy of silver-conjugated CNPs as a coating for titanium dental implants. They reported that this coating had sound inhibitory effect on proliferation of *Streptococcus mutans* and *Porphyromonas gingivalis*. Their results were in agreement with the present findings regarding optimal antibacterial activity of chitosan, although the type of microorganisms differed in the two studies. Saffarpour et al.⁹ compared the effects of Er: YAG laser, PDT with ICG and diode laser, toluidine blue, LED, and 2% CHX on *A. actinomycetemcomitans* on SLA implants. They demonstrated that aPDT with ICG and 810 nm diode laser with 300 mW power significantly decreased the colony count. Also, CHX was the most effective among all tested modalities. Their results regarding the optimal efficacy of aPDT were in accordance with the present findings; however, they did not use NPs; while, in the present study, aPDT

with ICG-loaded CNPs was as effective as CHX. Finally, it may be stated that using positively charged CNPs as a carrier for ICG significantly enhanced the decontamination efficacy of aPDT.

Bacteria in a biofilm are considerably more resistant to treatments compared to their planktonic form due to the protective nature of the biofilm matrix, which hinders penetration of therapeutic agents and protects the bacteria against the immune system of the host⁴¹. Thus, the biofilm form of *A. actinomycetemcomitans* was used in the present study to better simulate the clinical setting.

In vitro design was the main limitation of this study, which limits the generalizability of the findings. Photosensitizers applied in vitro are easy to control and can be uniformly applied. However, distribution of photosensitizer in vivo may be affected by tissue perfusion, saliva, or biofilm matrix. Also, the laser wavelength and energy density should be more precisely controlled in vivo due to tissue absorption and beam scattering in tissues. Also, aPDT is an oxygen-dependent phenomenon and well oxygenated media could be prepared in vitro. There are no host interactions and controlled, reproducible conditions can be prepared in vitro. In vitro models do not put live subjects at risk. However, they cannot capture the inherent complexity of organ systems and the internal environment of the human body. Scientific hypotheses must demonstrate their safety through in vitro experiments before being applied to humans^{42,43}. Also, only one type of photosensitizer, one type of microorganism, and one laser wavelength were assessed in the current study. Future studies are required on the efficacy of aPDT with different photosensitizers loaded on CNPs against other microorganisms in peri-implantitis by using different low-level laser wavelengths. Furthermore, the efficacy of other nanoparticles as a carrier for photosensitizers may be investigated in future studies. Finally, animal studies and subsequent clinical trials are required to verify the present findings in the clinical setting.

Conclusion

This study demonstrated that aPDT with ICG-loaded CNPs significantly reduced the *A. actinomycetemcomitans* colony count on dental implants, showing comparable efficacy to CHX.

While the in vitro results are promising, further clinical trials are necessary to confirm the effectiveness of this treatment in a real-world clinical setting.

Data availability

The data are in the “supplementary” file.

Received: 13 February 2025; Accepted: 11 August 2025

Published online: 01 October 2025

References

- Berglundh, T. et al. Peri-implant diseases and conditions: consensus report of workgroup 4 of the 2017 world workshop on the classification of periodontal and Peri-Implant diseases and conditions. *J. Clin. Periodontol.* **45** (Suppl 20), S286–S291 (2018).
- Misch, C. E. et al. Implant success, survival, and failure: the International Congress of Oral Implantologists (ICOI) Pisa consensus conference. *Implant Dent.* **17** (1) 5–15. (2008).
- Becker, W., Sennerby, L., Bedrossian, E., Becker, B. E. & Lucchini, J. P. Implant stability measurements for implants placed at the time of extraction: a cohort, prospective clinical trial. *J. Periodontol.* **76** (3), 391–397 (2005).
- Serino, G. & Ström, C. Peri-implantitis in partially edentulous patients: association with inadequate plaque control. *Clin. Oral Implants Res.* **20** (2), 169–174 (2009).
- Khammissa, R., Feller, L., Meyerov, R. & Lemmer, J. Peri-implant mucositis and periimplantitis: clinical and histopathological characteristics and treatment. *SADJ* **67** (3), 122–126 (2012).
- Papi, P. et al. Peri-implant diseases and metabolic syndrome components: a systematic review. *Eur. Rev. Med. Pharmacol. Sci.* **22**, 866–875 (2018).
- Azizi, B. et al. Antimicrobial efficacy of photodynamic therapy and light-activated disinfection against bacterial species on titanium dental implants. *Int. J. Oral Maxillofac. Implants.* **33** (4), 831–837 (2018).
- Rocuzzo, A., De Ry, S. P., Sculean, A., Rocuzzo, M. & Salvi, G. E. Current approaches for the non-surgical management of peri-implant diseases. *Curr. Oral Health Rep.* **7**, 274–282 (2020).
- Saffarpour, A. et al. Bactericidal effect of erbium-doped yttrium aluminum Garnet laser and photodynamic therapy on *Aggregatibacter actinomycetemcomitans* biofilm on implant surface. *Int. J. Oral Maxillofac. Implants.* **31** (3), e71–e78 (2016).
- Herrera, D. et al. Prevention and treatment of peri-implant diseases—The EFP S3 level clinical practice guideline. *J. Clin. Periodontol.* **50** (Suppl 26), 4–76 (2023).
- Renvert, S., Roos-Jansäker, A. M. & Claffey, N. Non-surgical treatment of peri-implant mucositis and peri-implantitis: a literature review. *J. Clin. Periodontol.* **35**, 305–315 (2008).
- Louropoulou, A., Slot, D. E. & Van der Weijden, F. A. Titanium surface alterations following the use of different mechanical instruments: a systematic review. *Clin. Oral Implants Res.* **23** (6), 643–658 (2012).
- Takasaki, A. A. et al. Application of antimicrobial photodynamic therapy in periodontal and peri-implant diseases. *Periodontol 2000.* **51** (1), 109–140 (2009).
- Hayek, R. R. et al. Comparative study between the effects of photodynamic therapy and conventional therapy on microbial reduction in ligature-induced peri-implantitis in dogs. *J. Periodontol.* **76** (8), 1275–1281 (2005).
- Madi, M. & Alagl, A. S. The effect of different implant surfaces and photodynamic therapy on periodontopathic bacteria using TaqMan PCR assay following peri-implantitis treatment in dog model. *Biomed. Res. Int.* **2018**, 7570105 (2018).
- Ghasemi, M., Etemadi, A., Nedaei, M., Chiniforush, N. & Pourhajbagher, M. Antimicrobial efficacy of photodynamic therapy using two different light sources on the titanium-adherent biofilms of *Aggregatibacter actinomycetemcomitans*: an in vitro study. *Photodiagnosis Photodyn Ther.* **26**, 85–89 (2019).
- Hart, I., Wells, C., Tsigarida, A. & Bezerra, B. Effectiveness of mechanical and chemical decontamination methods for the treatment of dental implant surfaces affected by peri-implantitis: A systematic review and meta-analysis. *Clin. Exp. Dent. Res.* **10** (1), e839 (2024).
- Rahman, B., Acharya, A. B., Siddiqui, R., Verron, E. & Badran, Z. Photodynamic therapy for peri-implant diseases. *Antibiot. (Basel).* **11** (7), 918 (2022).
- Allamyradov, Y. et al. Photodynamic therapy review: past, present, future, opportunities and challenges. *Photochem* **4** (4), 434–461 (2024).

20. Barbato, L. et al. Clinical efficacy of adjunctive methods for the non-surgical treatment of peri-implantitis: a systematic review and meta-analysis. *BMC Oral Health*. **23** (1), 375 (2023).
21. Yan, R., Zhan, M., Xu, J. & Peng, Q. Functional nanomaterials as photosensitizers or delivery systems for antibacterial photodynamic therapy. *Biomater. Adv.* **159**, 213820 (2024).
22. Bekmukhametova, A. et al. Photodynamic therapy with nanoparticles to combat microbial infection and resistance. *Nanoscale* **12** (41), 21034–21059 (2020).
23. Pourhajibagher, M., Hosseini, N., Boluki, E., Chiniforush, N. & Bahador, A. Photoelimination potential of Chitosan nanoparticles-indocyanine green complex against the biological activities of acinetobacter baumannii strains: a preliminary in vitro study in burn wound infections. *J. Lasers Med. Sci.* **11** (2), 187–193 (2020).
24. Rad, M. R., Pourhajibagher, M., Rohn, A. R., Barikani, H. R. & Bahador, A. Effect of antimicrobial photodynamic therapy using indocyanine green doped with Chitosan nanoparticles on biofilm Formation-Related gene expression of Aggregatibacter actinomycetemcomitans. *Front. Dent.* **16** (3), 187–193 (2019).
25. Chen, R. et al. Near-IR-triggered photothermal/photodynamic dual-modality therapy system via Chitosan hybrid nanospheres. *Biomaterials* **34** (33), 8314–8322 (2013).
26. Zhao, Y., Pu, R., Qian, Y., Shi, J. & Si, M. Antimicrobial photodynamic therapy versus antibiotics as an adjunct in the treatment of periodontitis and peri-implantitis: A systematic review and meta-analysis. *Photodiagnosis Photodyn Ther.* **34**, 102231 (2021).
27. Sheokand, N. et al. Use of antimicrobial photodynamic therapy as an adjunct in the treatment of Peri-Implantitis: A prospective study with 24 months follow up. [Journal name]. [Year];[Volume(Issue)]:[Page range]. [Add details if available].
28. Sahrman, P. et al. The Microbiome of peri-implantitis: a systematic review and meta-analysis. *Microorganisms* **8** (5), 661 (2020).
29. Sayar, F., Ghamari, N., Chiniforush, N., Bahador, A. & Fekrazad, R. Efficacy of antimicrobial photodynamic therapy for elimination of Aggregatibacter actinomycetemcomitans biofilm on Laser-Lok titanium discs. *Photodiagnosis Photodyn Ther.* **27**, 462–466 (2019).
30. Kamalou, A. M., Sayar, F. & Iranpour, B. Effect of antibacterial photodynamic therapy with Chitosan nanoparticles on Aggregatibacter actinomycetemcomitans. *Photodiagnosis Photodyn Ther.* **45**, 103996 (2024).
31. Sreekumar, S., Goycoolea, F. M., Moerschbacher, B. M. & Rivera-Rodriguez, G. R. Parameters influencing the size of chitosan-TTP nano-and microparticles. *Sci. Rep.* **8** (1), 4695 (2018).
32. Pourhajibagher, M., Chiniforush, N., Ghorbanzadeh, R. & Bahador, A. Photo-activated disinfection based on indocyanine green against cell viability and biofilm formation of Porphyromonas gingivalis. *Photodiagnosis Photodyn Ther.* **17**, 61–64 (2017).
33. Miles, A. A., Misra, S. S. & Irwin, J. O. The Estimation of the bactericidal power of the blood. *J. Hyg. (Lond)*. **38** (6), 732–749 (1938).
34. Mahmut, Z. et al. Medical applications and advancement of near infrared photosensitive indocyanine green molecules. *Molecules* **28** (16), 6085 (2023).
35. Shi, E. et al. Self-assembled nanoparticles containing photosensitizer and polycationic brush for synergistic photothermal and photodynamic therapy against periodontitis. *J. Nanobiotechnol.* **19** (1), 413 (2021).
36. Karimi, M. R., Montazeri, M., Harandi, M. & Aghazadeh, L. Effect of photodynamic therapy using toluidine blue on Eikenella corrodens and Aggregatibacter actinomycetemcomitans biofilms adhered to titanium discs: an in vitro study. *J. Res. Dent. Maxillofac. Sci.* **3** (4), 18–25 (2018).
37. Giannelli, M., Chellini, F., Margheri, M., Tonelli, P. & Tani, A. Effect of chlorhexidine digluconate on different cell types: a molecular and ultrastructural investigation. *Toxicol. Vitro.* **22** (2), 308–317 (2008).
38. Brunello, G. et al. The effects of three chlorhexidine-based mouthwashes on human osteoblast-like SaOS-2 cells. An in vitro study. *Int. J. Mol. Sci.* **22** (18), 9986 (2021).
39. Nagahara, A. et al. Antimicrobial photodynamic therapy using a diode laser with a potential new photosensitizer, indocyanine green-loaded nanospheres, May be effective for the clearance of Porphyromonas gingivalis. *J. Periodontal Res.* **48** (5), 591–599 (2013).
40. Divakar, D. D. et al. Enhanced antimicrobial activity of naturally derived bioactive molecule Chitosan conjugated silver nanoparticle against dental implant pathogens. *Int. J. Biol. Macromol.* **108**, 790–797 (2018).
41. Shahmoradi, S. et al. The application of selenium nanoparticles for enhancing the efficacy of photodynamic inactivation of planktonic communities and the biofilm of Streptococcus mutans. *BMC Res. Notes.* **15** (1), 84 (2022).
42. Jonathan Dornell. In Vivo vs In Vitro: Definition, Pros and Cons. Technology Networks 2021 July 1. <https://www.technologynetworks.com>
43. Grinholc, M. et al. Antimicrobial photodynamic therapy with fulleropyrrolidine: photoinactivation mechanism of *Staphylococcus aureus*, in vitro and in vivo studies. *Appl. Microbiol. Biotechnol.* **99**, 4031–4043 (2015).

Acknowledgements

The authors would like to thank Dr. Nasim Chiniforush, Dr. Mohammad Javad Kharrazi Fard, Dr. Moradikhah for their cooperation in conduction of this study.

Author contributions

All authors have made substantial contributions to conception and design of the study. FS, SB, have been involved in writing the main manuscript, data collection and data analysis. FS, MRK, SB have been involved in data interpretation, drafting the manuscript and revising it critically and have given final approval of the version to be published.

Declarations

Competing interests

The authors declare no competing interests.

Additional information

Supplementary Information The online version contains supplementary material available at <https://doi.org/10.1038/s41598-025-15871-3>.

Correspondence and requests for materials should be addressed to F.S. or M.R.K.

Reprints and permissions information is available at www.nature.com/reprints.

Publisher's note Springer Nature remains neutral with regard to jurisdictional claims in published maps and institutional affiliations.

Open Access This article is licensed under a Creative Commons Attribution-NonCommercial-NoDerivatives 4.0 International License, which permits any non-commercial use, sharing, distribution and reproduction in any medium or format, as long as you give appropriate credit to the original author(s) and the source, provide a link to the Creative Commons licence, and indicate if you modified the licensed material. You do not have permission under this licence to share adapted material derived from this article or parts of it. The images or other third party material in this article are included in the article's Creative Commons licence, unless indicated otherwise in a credit line to the material. If material is not included in the article's Creative Commons licence and your intended use is not permitted by statutory regulation or exceeds the permitted use, you will need to obtain permission directly from the copyright holder. To view a copy of this licence, visit <http://creativecommons.org/licenses/by-nc-nd/4.0/>.

© The Author(s) 2025